



# Laser Ablation Ionization Mass Spectrometry: A Space Prototype System for *In Situ* Sulphur Isotope Fractionation Analysis on Planetary Surfaces

Andreas Riedo<sup>1\*</sup>, Valentine Grimaudo<sup>1</sup>, Joost W. Aerts<sup>2</sup>, Rustam Lukmanov<sup>1</sup>, Marek Tulej<sup>1</sup>, Peter Broekmann<sup>3</sup>, Robert Lindner<sup>4</sup>, Peter Wurz<sup>1</sup> and Pascale Ehrenfreund<sup>5,6</sup>

<sup>1</sup>Space Research and Planetary Sciences, Physics Institute, University of Bern, Bern, Switzerland, <sup>2</sup>Molecular Cell Physiology, Faculty of Earth and Life Sciences, VU University Amsterdam, Amsterdam, Netherlands, <sup>3</sup>Interfacial Electrochemistry Group, Department of Chemistry, Biochemistry and Pharmaceutical Sciences, University of Bern, Bern, Switzerland, <sup>4</sup>Life Support and Physical Sciences Instrumentation Section, European Space Agency ESTEC, Noordwijk, Netherlands, <sup>5</sup>Laboratory for Astrophysics, Leiden Observatory, Leiden University, Leiden, Netherlands, <sup>6</sup>Space Policy Institute, George Washington University, Washington, DC, United States

## OPEN ACCESS

### Edited by:

Isik Kanik,  
NASA Jet Propulsion Laboratory  
(JPL), United States

### Reviewed by:

Josep M. Trigo-Rodríguez,  
Consejo Superior de Investigaciones  
Científicas (CSIC), Spain  
Svatopluk Civiš,  
J. Heyrovsky Institute of Physical  
Chemistry (ASCR), Czechia

### \*Correspondence:

Andreas Riedo  
andreas.riedo@unibe.ch

### Specialty section:

This article was submitted to  
Astrobiology,  
a section of the journal  
Frontiers in Astronomy and Space  
Sciences

**Received:** 16 June 2021

**Accepted:** 05 October 2021

**Published:** 05 November 2021

### Citation:

Riedo A, Grimaudo V, Aerts JW, Lukmanov R, Tulej M, Broekmann P, Lindner R, Wurz P and Ehrenfreund P (2021) Laser Ablation Ionization Mass Spectrometry: A Space Prototype System for *In Situ* Sulphur Isotope Fractionation Analysis on Planetary Surfaces. *Front. Astron. Space Sci.* 8:726373. doi: 10.3389/fspas.2021.726373

The signatures of element isotope fractionation can be used for the indirect identification of extant or extinct life on planetary surfaces or their moons. Element isotope fractionation signatures are very robust against the harsh environmental conditions, such as temperature or irradiation, which typically prevail on solar system bodies. Sulphur is a key element for life as we know it and bacteria exist, such as sulphur reducing bacteria, that can metabolize sulphur resulting in isotope fractionations of up to  $-70\%$   $\delta^{34}\text{S}$ . Geochemical processes are observed to fractionate up to values of  $-20\%$   $\delta^{34}\text{S}$  hence, fractionation exceeding that value might be highly indicative for the presence of life. However, the detection of sulphur element isotope fractionation *in situ*, under the assumption that life has existed or still does exist, is extremely challenging. To date, no instrument developed for space application showed the necessary detection sensitivity or measurement methodology for such an identification. In this contribution, we report a simple measurement protocol for the accurate detection of sulphur fractionation  $\delta^{34}\text{S}$  using our prototype laser ablation ionization mass spectrometer system designed for *in situ* space exploration missions. The protocol was elaborated based on measurements of five sulphur containing species that were sampled at different Mars analogue field sites, including two cave systems in Romania and the Río Tinto river environment in Spain. Optimising the laser pulse energy of our laser ablation ionization mass spectrometer (LIMS) allowed the identification of a peak-like trend of the  $^{34}\text{S}/^{32}\text{S}$  ratio, where the maximum, compared to internal standards, allowed to derive isotope fractionation with an estimated  $\delta^{34}\text{S}$  accuracy of  $\sim 2\%$ . This accuracy is sufficiently precise to differentiate between abiotic and biotic signatures, of which the latter, induced by, e.g., sulphate-reducing microorganism, may fractionate sulphur isotopes by more than  $-70\%$   $\delta^{34}\text{S}$ . Our miniature LIMS system, including the discussed measurement protocol, is simple and

can be applied for life detection on extra-terrestrial surfaces, e.g., Mars or the icy moons like Europa.

**Keywords:** LIMS, sulphur isotope fractionation, biosignature, mass spectrometry, space instrument, life, laser ablation

## INTRODUCTION

The chemical analysis of sulphur containing solids is of importance to various scientific research disciplines, ranging from the geochemistry of Earth or Mars (Ding et al., 2015), for a better understanding of the formation process of our solar system via chemical analysis of meteoritic material (Trigo-Rodríguez et al., 2015; Visser et al., 2019), to the identification of signatures of life produced by bacteria. Sulphur isotope studies on solids collected from various locations on Earth provided insights into various geochemical processes that shaped our Earth atmosphere and crust, such as atmospheric chemistry and crustal recycling. It allowed to divide Earth history in three different stages with the great oxidation event at ~2.45 to 2.0 Ga (Farquhar et al., 2000; Farquhar et al., 2002; Farquhar and Wing, 2003). Sulphur is also relevant beyond our Earth; it is for example a key element on Mars. Sulphur is an abundant element on Mars and the sulphur cycle is of utmost importance as it defines, e.g., Mars's differentiation and geochemical processes, climate history, and current and past habitability (King and McLennan, 2010; Ding et al., 2015). In astrobiology, fractionated sulphur isotopes are proposed as robust biomarkers for the detection of signatures of life (Chela-Flores, 2018), because, in comparison to biomolecules (amino acids, lipids, etc.), such markers are much less affected by the harsh temperature, radiation and ionization conditions typically present on solar system objects which lack a protecting atmosphere and electromagnetic shielding. Such sulphur fractionated isotope signatures may be preserved on Mars (Chela-Flores, 2018), potentially in close vicinity to ancient lakes, where life may have flourished (Chela-Flores, 2010; Chela-Flores et al., 2014), on the icy moons of Jupiter and Saturn, most probably on Europa, Enceladus or Ganymede (Chela-Flores, 2006; Chela-Flores and Kumar, 2008), and even beyond our outer solar system (Chela-Flores, 2017). Sulphur fractionation is described via the following equation

$$\delta^{34}\text{S} = \left( \frac{\left(\frac{^{34}\text{S}}{^{32}\text{S}}\right)_{\text{Sample}} - \left(\frac{^{34}\text{S}}{^{32}\text{S}}\right)_{\text{Ref}}}{\left(\frac{^{34}\text{S}}{^{32}\text{S}}\right)_{\text{Ref}}} \times 1000 \right)$$

where  $\left(\frac{^{34}\text{S}}{^{32}\text{S}}\right)_{\text{Ref}}$  and  $\left(\frac{^{34}\text{S}}{^{32}\text{S}}\right)_{\text{Sample}}$  denote the measured ratio of a given sulphur reference and sample of interest, respectively.

Sulphur-reducing bacteria metabolise sulphur by reducing sulphates to sulfides, whereby the lighter S-isotope  $^{32}\text{S}$  is favoured in the process (sulphates are depleted while sulfides are enriched in  $^{32}\text{S}$ ). Therefore, the sulphur isotopes are of special interest to space research in general and astrobiology in particular. Natural populations on Earth were observed to fractionate sulphur isotopes up to a level of about  $\delta^{34}\text{S} = -70\%$ . These high levels of fractionation are clearly indicative of life metabolism, because geochemical processes can fractionate

sulphur isotopes only up to about 20‰  $\delta^{34}\text{S}$ . If such reducers have ever existed on Mars, or still exist in the recently discovered subglacial liquid reservoir at the south pole (Orosei et al., 2018), biomarkers might (still) be present and detectable. The liquid oceans of the Jovian and Galilean satellites Europa and Enceladus may host such reducers as well and the patchy sulphur deposits on the ice shells may host such biomarkers. However, robust and simple measurement techniques are missing for *in situ* operation that have the capability to provide reliable data on sulphur isotopes with sufficiently high accuracy and precision at the per mill level for  $\delta^{34}\text{S}$ .

How life emerged on Earth, and potentially on other solar system bodies is still under big discussion (see, e.g., Rotelli et al., 2016; Cabedo et al., 2021) and references therein. One of the theories is that organic matter was delivered by meteorites to the early Earth and the local conditions allowed the formation of more complex molecular structures required for the emergence of life. Research on chondrites, a class of meteorites coming from undifferentiated bodies (never melted, limited thermal and chemical alteration) and believed to be one of the most pristine material of our Solar System (Cabedo et al., 2021), are of particular interest for this topic. Previous studies identified and quantified amino acids, important building blocks of life (Aerts et al., 2014), in various meteorites, such as CM2 and CR2 types (Cronin and Pizzarello 1983; Akira et al., 1985; Martins et al., 2007a; Martins et al., 2007b; Trigo-Rodríguez et al., 2015). Therefore space mission aim to find a set of amino acids on extra-terrestrial bodies that are also found in both biological process on Earth and meteoritic material (e.g., Hand et al., 2017).

Sulphur isotopes studies on meteorites, including the well-known Martian meteorite Allan Hills 84001 have been conducted (Shearer et al., 1996). Such measurements aim, e.g., to find fractionation patterns which might indicate biological activity (Kaplan and Hulston 1966; Shearer et al., 1996). However, in the investigated meteorites, no clear evidence was observed that would point to biological activity. Neither in the case of the Martian meteorite Allan Hills 84001 (positive  $\delta^{34}\text{S}$  values for pyrite lower than about +8‰ were observed), nor in the contribution from (Kaplan and Hulston 1966), who investigated twenty different meteorites ( $\delta^{34}\text{S}$  values in the range of -2.5‰ to +5.5‰ were observed). However, the non-detection of biological patterns (sulphur fractionation that can be solely induced by biological process) in, e.g., the Martian meteorite Allan Hills 84001 does not necessarily conclude about the existence or non-existence of past or present biological activity on Mars. Therefore, *in situ* investigation on Mars surface and subsurface samples are of high importance as such measurements do provide a more comprehensive look into the evolution of Mars and the possibility for trace life signatures.

In this contribution, we describe a novel measurement protocol for the accurate quantification of sulphur fractionation  $\delta^{34}\text{S}$  with accuracy at the level of  $\sim 2\%$  using our miniature laser ablation ionization mass spectrometry (LIMS) system, a prototype for *in situ* space research. Measurements were conducted on five different Mars analogue materials collected all at field sites mimicking certain environmental parameters of Mars' history and current environments that might exist beneath the surface of Mars. Two of these specimens, showing an enriched and depleted  $\delta^{34}\text{S}$  value, respectively, were used as internal standard for the  $\delta^{34}\text{S}$  calibration of the other three samples. The application of a sweep of laser pulse energies allowed the identification of most appropriate measurement settings for the accurate quantification of sulphur fractionation, which, to our best current knowledge, was so far not feasible using a space prototype LIMS system. The herein proposed measurement protocol is robust, simple, and sufficiently accurate for future *in situ* applications. It has clearly a high potential to provide valuable information on geochemical processes which occurred on solar system body surfaces (see discussion above). Furthermore, this protocol might be applied in the future for the identification of life based on sulphur metabolism.

## MATERIALS AND METHODS

### Field Site Description

For the elaboration of the measurement protocol five samples from three different field sites were investigated; three samples (named RT1, RT2, RT6) from the river Río Tinto, Spain (Amils et al., 2007), one from the Movile Cave (named MC) (Chen et al., 2009; Kumaresan et al., 2014; Kumaresan et al., 2018) and one from the Sulphur Cave (named SC) (Sarbu et al., 2018), that are both located in Romania. These three field sites were selected for measurements because they reflect some environment conditions that occurred, or may still exist, on current Mars.

The Río Tinto river (Iberian Pyritic Belt) environment in Spain is a special Mars analogue site that is well-known to the astrobiology community. The river is highly acidic (mean pH value of only 2.3), contains many heavy metals (Fe, Cu, Zn, As, among others) at high concentrations, high levels of ferric iron and sulphates as a result of the bio-oxidation of pyrite, and shows a high level of various microbial life. The Iberian Pyritic Belt is known to be one of the largest natural supplies on Earth of metallic sulphides. Concerning the sulphur cycle of the ecosystem, only acidithiobacillus *ferrooxidans* (sulphur oxidizing bacteria (SOB)), which is a chemolithotroph, is present; some sulphur reducing bacteria (SRB) have been identified at some locations at the river but play only a minor role. The high abundance of SOB results in the observed high concentration of sulphates in that river system (Amils et al., 2007).

Movile Cave is located few kilometers away from the black sea, near the town of Mangalia, Romania, and is about 21 m below ground. It was discovered in 1986 during the construction of an artificial shaft. The cave's ecosystem primarily depends on chemosynthesis and shows strong similarities to deep-sea

hydrothermal vents. The cave system is composed of an upper dry section, which connects to the deeper submerged passages that are flooded by mesothermal waters originating from an underlying sulfidic aquifer. Several airbells exist deeper into the cave which are separated from the upper section of the cave by the submerged passages (see, e.g., Fig. 1 in Kumaresan et al. (2014)). The water flowing through the cave contains high levels of  $\text{H}_2\text{S}$  (0.2–0.3 mM),  $\text{CH}_4$  (0.02 mM),  $\text{NH}_4^+$  (0.2–0.3 mM), and has a constant pH level of 7.4 at a constant temperature 20.9°C. The temperature of the atmosphere in the cave near the submerged section is also around 21°C and contains elevated levels of  $\text{CO}_2$  and high humidity. The sample was collected on the location where the flooded part of the cave meets with the upper dry section. A rich and diverse microbial community is present in the cave with high numbers of SOB and SRB, among many others. A more detailed description of this cave system can be found in, e.g., Chen et al. (2009), Kumaresan et al. (2014), Kumaresan et al. (2018).

Sulphur Cave (N46.119764; E25.948640) in Romania is another extreme environment where microbial life is present in high numbers. This cave is located on the Ciomadul volcanic environment, in the east Carpathian Mountains, Romania (Sarbu et al., 2018), at an altitude of about 1 km above sea level. The cave system is about 14 m long, and approximately the first 7 m can be accessed by humans. The cave system contains a sharp atmospheric interface, a gas chemocline, where air floats on top the heavier volcanic gases such as  $\text{CO}_2$  (97–98%),  $\text{CH}_4$ , and  $\text{H}_2\text{S}$  (see Fig. 3 in Sarbu et al., (2018)). The wall below and at this  $\text{CO}_2$ - $\text{H}_2\text{S}$ /air interface are fully covered with  $\text{S}^0$  and  $\text{H}_2\text{SO}_4$  (from sulphur oxidation). At the interface, the pH is below 1 and is inhabited by prominent microbial biofilms. It is believed that the microbial community survives via oxidation of  $\text{H}_2\text{S}$  and  $\text{S}^0$ , although other mechanisms may also occur. This environment represents an analogue site to subsurface, near volcanic environments on Mars or other solar system objects. Moreover, the environment below the interface has similarities to the Martian atmosphere in terms of relative abundance of  $\text{CO}_2$ ,  $\text{N}_2$ , and  $\text{O}_2$ . The microbial community investigated at this interface level is much lower in diversity, with Mycobacteria dominating the communities (above the interface) followed by some minor groups such as Acidithiobacillus (bacteria, below the interface), Acidmyces (fungi, at the interface), and Ferroplasmaceae (Archea). Acidithiobacillus is of interest because they can grow chemoautotroph- and anaerobically, and are capable of oxidizing the available sulphur compounds. Full description of this field site can be found in Sarbu et al., (2018).

The samples selected for this study differ from each other in their sulphur content, ranging from 5.7 to 96.5% (weight abundance), and in their  $\delta^{34}\text{S}$  sulphur isotope fractionation from  $-7.1$  to  $+8.6$ . Both the isotope fractionation and sulphur content were measured externally with a state-of-the-art isotope measurement setup hosted at Lancaster University, United Kingdom (discussed in the follow).

### Sample Preparation

The raw sample material was dried overnight at room temperature in Eppendorf tubes (Figure 1A) in an evacuated

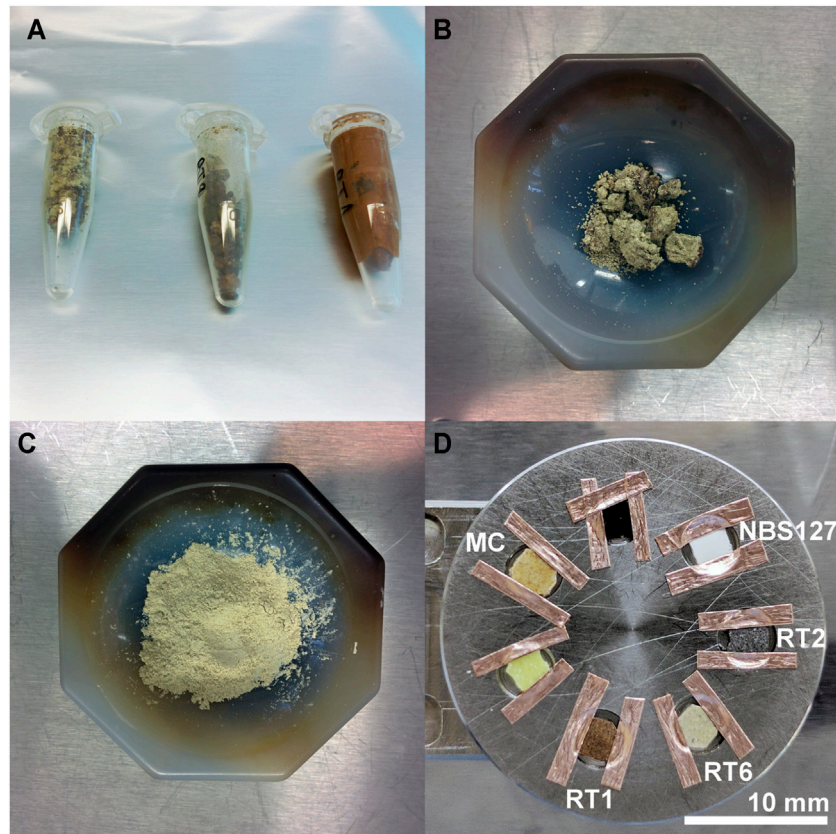


**FIGURE 1** | Preparation procedure applied to the sample materials prior to the chemical analysis. **(A)** Sample materials are filled in Eppendorf tubes for drying using a dedicated centrifuge-dryer system, **(B)** Sample material of granular appearance after the drying, **(C)** Obtained fine powder material after the grinding of the material shown in panel **(B,D)** Samples cut from pellets of the pressed materials; for the chemical analysis using LIMS samples were fixed on the sample holder using conductive Cu tape (suitable for UHV applications).

(at mbar level) centrifuge-dryer system (CentriVap Centrifugal concentrator/ColdTrap system, LabConco). The dry material was subsequently ground into fine powder (**Figures 1B,C**) from which about 200 mg of each sample was finally pressed (5 min at about 13 tons) into pellets. The pellets have a diameter of about 1 cm and a thickness in the range of about (0.5–1) mm. For LIMS analysis, the pellets were further cut into round disks with diameters of about 3–4 mm, to allow several samples to be placed on the same LIMS sample holder (**Figure 1D**). The sample holder presented in **Figure 1D** supports the three investigated samples from Río Tinto (named RT1, RT2, and RT6) and the sample from Movile Cave (MC). The very low pH sample from the Sulphur Cave was placed on an extra sample holder. Cu tape, suitable for ultra-high-vacuum applications, was used to fix the samples on the LIMS sample holder. LIMS measurements were conducted on the most central part of the samples.

## Energy Dispersive X-Ray Spectroscopy Measurements

Scanning electron microscopy (SEM) and corresponding Energy Dispersive X-ray (EDX) spectroscopy mapping measurements

(Hitachi, S300N instrument, working distance  $\sim 17.1$  mm, acceleration voltage 25 kV, image size  $512 \times 384$  px) were conducted with the aim to study the surface morphology and porosity (e.g., voids, depressions etc.) of the pressed sulphur samples (**Figure 1D**). Note that the mesoscale morphology and porosity of the target samples is of high relevance also to the LIMS measurement. Because the field-of-depth of our current LIMS system is at the order of tens of micrometres laser ablation from an uneven surface (e.g., due to sub-surface voiding at the location of laser ablation) might lead to unintended and significant variations in the measured MS intensity; e.g., the sample surface might be out of the laser focus.

## State-of-the Art Sulphur Isotope Analysis

The dry and fine powder material (**Figure 1C**) was sent to the Lancaster laboratory for highly accurate sulphur abundance and isotope analysis. The received isotope values were taken as reference values for the LIMS measurements.

Sulphur abundance and isotope ratio measurements were carried out at Lancaster University, England by the group of Prof. Dr. Wynn (Wynn et al., 2014). The received powder material (**Figure 1C**) was first dried again at  $60^\circ\text{C}$  for 4 h before adding the material into tin capsules. The added

**TABLE 1** | Sulphur abundance and isotope ratio measurements conducted at Lancaster University. Each sample was delivered in powdered form and a minimum of two measurements were performed for sulphur isotope measurements. Four isotope standards were used for calibration of the measurements (details in the text).

Location	Sample ID	Sulphur abundance [weight %]	$\delta^{34}\text{S}_{\text{mean}}$	$\delta^{34}\text{S}$
Rio Tinto, Spain	RT1	5.7	7.89	7.82 7.96
	RT2	30.2	8.63	8.64 8.62
	RT6	14.9	6.88	6.94 6.82
Movile Cave, Romania	MC	15.5	3.61	3.35 3.74 3.74
Sulphur Cave, Romania	SC	96.5	-7.12	-7.04 -7.16 -7.17

material was variable and was within the range of about 0.25–16 mg. To improve the combustion vanadium pentoxide was added to the capsules. The material was analysed by a continuous-flow-isotope-ratio mass spectrometer using an Isoprime100 mass spectrometer coupled with Elementar Vario PYROcube elemental analyser. The samples were combusted in the element analyser at 1,120°C and the generated SO<sub>2</sub> was analysed on the Isoprime spectrometer. For the quantification of sulphur abundance and isotope ratio various certified international standards were used, including IAEA SO<sub>6</sub>, SO<sub>5</sub> and NBS 127, along with a custom-made LEC laboratory standard named MSLG. All the standards were BaSO<sub>4</sub> materials. An overview of the measurement results is given in **Table 1**.

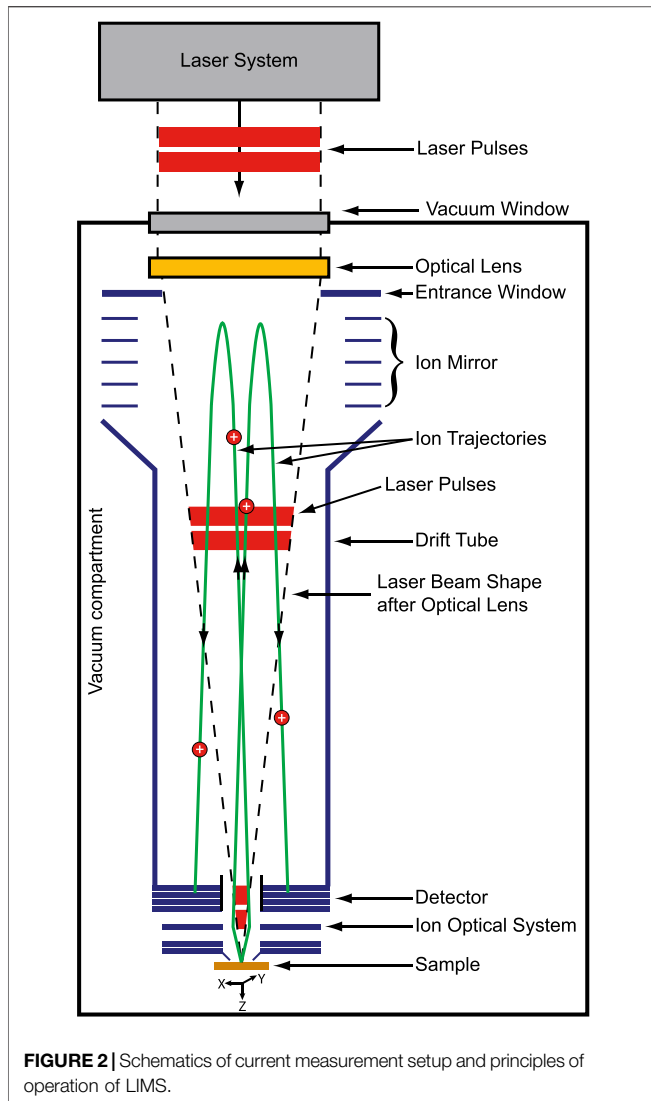
## Laser Ablation Ionization Mass Spectrometry

Laser ablation ionization mass spectrometric (LIMS) measurements were conducted using the laser ablation ionization prototype mass spectrometric system built at the University of Bern. The system was originally designed for the *in situ* chemical analysis of solids (elements and isotopes) on planetary bodies. Detailed information about the design and principles of operation can be found in previous publications, see, e.g., Riedo et al., 2013a; Riedo et al., 2013b; Grimaudo et al., 2015; Neubeck et al., 2015; Tulej et al., 2015; Grimaudo et al., 2017; Stevens et al., 2019; Riedo et al., 2020; Tulej et al., 2021. In the following only a brief description about the measurement principles is given.

The LIMS system consists of a miniature reflectron-type time-of-flight mass spectrometer (RTOF, analyzer with dimensions of 160 mm × Ø 60 mm, installed within vacuum chamber with typical base pressure of mid 10<sup>-8</sup> mbar) which is coupled to a femtosecond laser system (wavelength  $\lambda$  = 775 nm, laser pulse repetition rate of 1 kHz, installed outside the vacuum chamber) for ablation and ionization of sample material. For the current studies, the ion source was operated in double pulse mode (the fundamental laser pulse is divided into two pulses with equal energy, with one delayed in

regard to the first laser pulse) to further enhance the ion production by post ionization of neutrals produced by the first laser pulse. The pulse delay for efficient post-ionization of the generated ablation plume was at the level of 20–30 ps. Further details about this double pulse ion source can be found in previous publications (Riedo et al., 2021; Tulej et al., 2018). The laser beam is focused through the mass analyzer towards the sample surface to spot sizes of ~10–20  $\mu\text{m}$  in diameter. The positive ions generated during the laser ablation and post-ionization process enter the mass analyzer, and are accelerated, confined and focused to the field-free drift path. At the ion mirror (reflectron), the ions are reflected towards the detector system by passing a second time the drift path. The schematics of the current measurement set-up and LIMS principles of operation are illustrated in **Figure 2**. TOF spectra are recorded with a high-speed measurement system (8 bit vertical dynamics, up to 4 GS/s), and an in house written software-suite was used for the data analysis that includes, e.g., signal integration, conversion of TOF to mass spectrum (Meyer et al., 2017). The sample holder is positioned below the mass analyzer on a three dimensional translation stage with micrometer position accuracy. A high-resolution microscope camera system is installed co-axially to the mass analyzer to allow accurate targeting of surface material. The camera system has a resolving power of 1  $\mu\text{m}$  (Wiesendanger et al., 2018).

On each sample, a laser irradiance campaign was conducted; the pulse energy was varied in the range of about 0.3–1.7  $\mu\text{J}$  (depending on the sample). For each instrument setting, measurements were conducted on a fresh surface location. Typically, 200–400 mass spectra files were saved on the host computer, each representing an accumulation of 50 single laser shot TOF spectra, realized with the onboard processing capabilities of the used measurement cards. Spectra showing poor mass resolution or reduced signal-to-noise-ratios (SNR) were not considered for data analysis. Typically, lower mass resolution is observed during ablation crater formation at the beginning of the measurement and at high pulse energies (space charge effects impacts the mass resolution), and reduced SNR at the later stage of ablation occurs, because the sample is not



adjusted actively to keep the material ablation in the focal plane. The recorded mass spectrometric measurements allow the element composition analysis of the samples which enables to derive accurately the sulphur isotope abundance. Note that the element analysis of the samples is on qualitative nature only. For true quantification of the element composition reference standards are required, which is not the scope of this study here.

Similar to the state-of-the-art sulphur isotope measurements conducted at Lancaster facilities (see section *State-of-the Art Sulphur Isotope Analysis*), it was originally planned to use the isotope sulphur isotope standard NBS 127 (see white sample on sample holder displayed in **Figure 1**) for the calibration of the recorded data of the cave and Río Tinto samples. However, it was challenging to find optimal ion optical settings for the recording of well-resolved mass spectra, which is a prerequisite for the subsequent data analysis. Therefore, it was decided to use the RT2 and the SC sample as internal reference samples. These two samples

were selected because both show extrema in their  $\delta^{34}\text{S}$  fractionation, required for  $\delta^{34}\text{S}$  normalization as suggested by NIST, and are highly abundant in sulphur (**Table 1**). Both are important aspects, and later especially for laser ablation techniques. Only samples highly abundant in species of interest should be used for quantification studies.

For the  $\delta^{34}\text{S}$  calibration using our LIMS system the normalization approach as discussed by NIST was used (see, e.g., NIST certificate for reference material 8557, NBS127, sulphur and oxygen isotope reference material) and slightly modified as follows:

$$\delta^{34}\text{S}_{\text{sample,cal}} = \delta^{34}\text{S}_{\text{ST1,cal}} + \left( \frac{{}^{34}\text{S}/{}^{32}\text{S}_{\text{sample,meas}} - {}^{34}\text{S}/{}^{32}\text{S}_{\text{ST1,meas}}}{\delta^{34}\text{S}_{\text{ST2,cal}} - \delta^{34}\text{S}_{\text{ST1,cal}}} \right) \times f,$$

where the normalization factor  $f$  is derived as follows:

$$f = \left( \delta^{34}\text{S}_{\text{ST2,cal}} - \delta^{34}\text{S}_{\text{ST1,cal}} \right) / \left( \frac{{}^{34}\text{S}/{}^{32}\text{S}_{\text{ST2,meas}} - {}^{34}\text{S}/{}^{32}\text{S}_{\text{ST1,meas}}}{\delta^{34}\text{S}_{\text{ST2,cal}} - \delta^{34}\text{S}_{\text{ST1,cal}}} \right),$$

where *meas* denotes measured values, *cal* calibrated values, ST1 and ST2 standards with high and low  $\delta^{34}\text{S}$  values (here the RT2 and SC samples) measured in Lancaster facilities (**Table 1**), and  ${}^{34}\text{S}$  and  ${}^{32}\text{S}$  denotes the measured peak area in the recorded TOF spectra.

## RESULTS

### EDX Measurements

In **Figure 3** the EDX mappings conducted on the five different samples are shown. In general, a uniform distribution of sulphur within the pressed powder material can be observed. This is further supported by the LIMS measurements where the sample position needed to be changed rarely due to low detected signal. Targeting a void using LIMS would result in a significant reduced signal due to the reduced material ablation. In such an event, the measurement has been repeated on a new sample location using the same instrument settings.

### LIMS Bulk Chemical Analysis

In **Figure 4**, the element composition analysis using LIMS of the samples RT1, RT2, RT6, MC, and SC is presented, within the mass to charge  $m/z$  range of 5–170. Each mass spectrum is an accumulation of 7,500 single shot spectra, saved into 150 spectra files on the host computer. For simplicity, the mass spectra displayed are normalized to their major abundant element isotope. Note that the shown mass spectra are not quantified (not purpose of this study), however, the composition can be discussed on a qualitative level, because all the spectra were recorded at comparable instrument settings. In comparison to the samples RT1, RT2, RT6, and SC a higher laser pulse energy was needed to be applied for the MC sample, which points to, e.g., harder sample material.

### LIMS Isotope Analysis

NIST suggests the use of a  ${}^{34}\text{S}$ -enriched (e.g., SRM 8555,  $\delta^{34}\text{S} = +22.62$ ) and depleted (e.g., SRM 8529,  $\delta^{34}\text{S} = -32.49$ ) standard for accurate quantification of the measured sulphur isotope

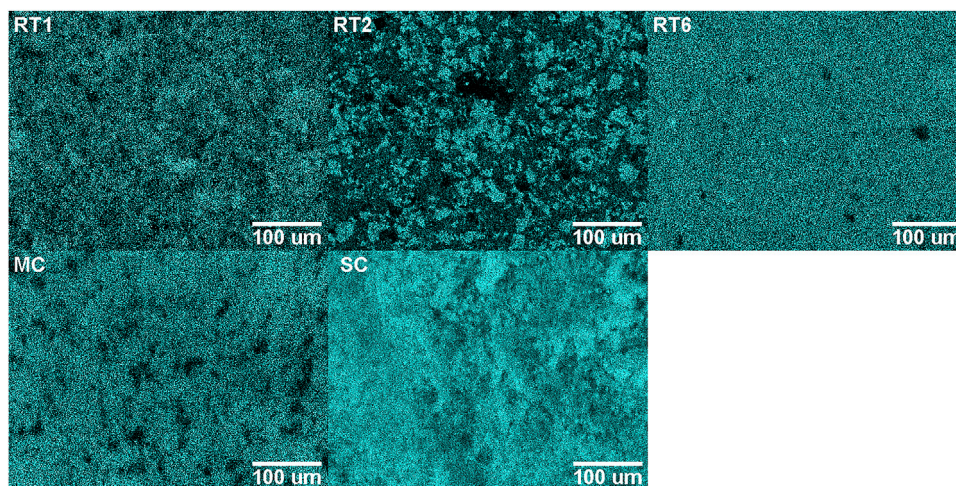


**FIGURE 3** | EDX measurements of the investigated sulphur samples. Shown is the sulphur signal. Brighter colour represents **higher** element abundance. In general, the sulphur content is well distributed within the investigated sample surface.

abundance of the sample of interest. Originally, it was planned to use NBS 127 (SRM 8557,  $\delta^{34}\text{S} = +21.17$ ) as the enriched standard, and using the RT2 sample with lower enrichment of  $^{34}\text{S}$  ( $\delta^{34}\text{S} = +8.63$ ). But because the physical-chemical composition of the NBS 127 is very different to the natural samples collected, which would require significant different instrument parameters for material ablation, we decided to use the samples RT2 ( $\delta^{34}\text{S} = +8.63$ , enriched) and SC ( $\delta^{34}\text{S} = -7.12$ , depleted) as internal standards for the calibration and normalization procedure discussed at the end of section *Laser Ablation Ionization Mass Spectrometry*. These two samples cover well the  $\delta^{34}\text{S}$  fractionation region of the samples investigated. Note that the state-of-the-art sulphur isotope measurements were performed with sub- $\delta^{34}\text{S}$  accuracy (Table 1), which is sufficiently accurate for our LIMS analysis, which shows accuracies at the  $\delta^{34}\text{S}$  level.

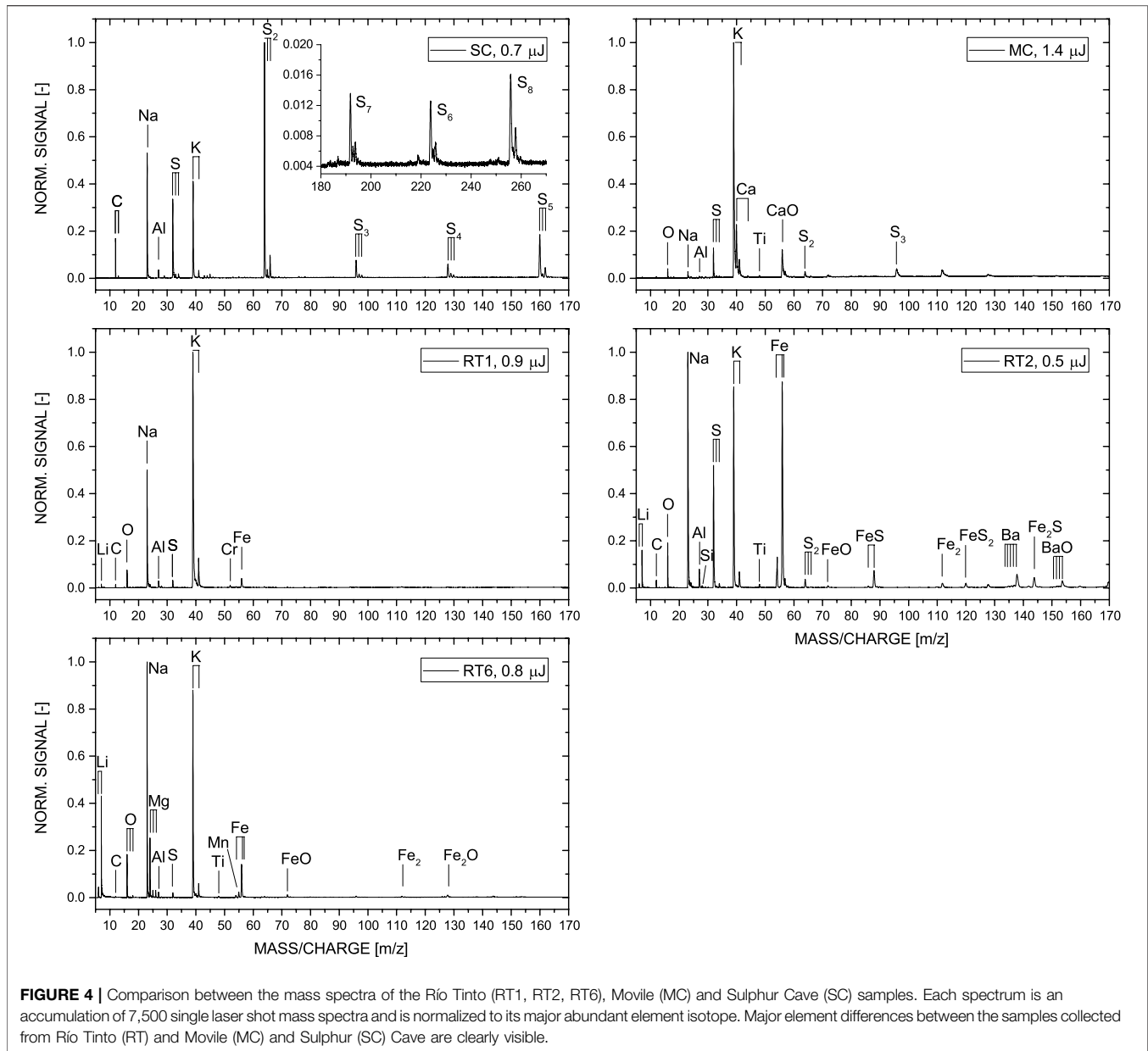
Figure 5 illustrates the detailed measurement campaign conducted on the RT2. On the left panel, the sulphur ratio  $^{34}\text{S}/^{32}\text{S}$  as a function of applied pulse energy is displayed. Here the pulse energies of  $\sim 0.3$ – $1.2 \mu\text{J}$  were applied. Each measurement was conducted on a fresh sample surface location, where up to 10,000 laser shots were fired, resulting in 10,000 recorded TOF spectra, accumulated in 200 files (each file corresponds to an accumulation of 50 single laser shot spectra). Optimal conditions, which in this study was a compromise between signal stability and mass resolution, were observed for an applied laser pulse energy of  $\sim 0.5 \mu\text{J}$ . This was the reason why up to six measurements were conducted at this same instrument setting (open, square symbols). The blue square data point at  $\sim 0.5 \mu\text{J}$  (Figure 5A) represents the average of all these six measurements, and this data point was used for  $\sim 0.5 \mu\text{J}$  to calculate the mean  $^{34}\text{S}/^{32}\text{S}$  ratio for all pulse energies of the entire campaign. The shown measurements in the left panel were conducted on two different days, indicated with first and second campaign. In the second measurement campaign pulse energies of up to  $\sim 1.2 \mu\text{J}$  were applied to the sample material. The two measurements displayed in purple showed a significant lower SNR of the sulphur isotopes which affects especially the appearance of  $^{34}\text{S}$ , resulting in a lower  $^{34}\text{S}/^{32}\text{S}$

ratio. Therefore these two measurements were not considered for the mean ratio analysis. Including all the measurements (using the mean for measurements conducted at  $\sim 0.5 \mu\text{J}$ , and neglecting the two measurements at elevated pulse energies) a mean  $^{34}\text{S}/^{32}\text{S}$  ratio of  $0.028 \pm 0.001$  was derived. The dashed grey area represents the mean  $^{34}\text{S}/^{32}\text{S}$  value  $\pm \sigma$ .

As discussed above, up to 200 accumulated spectra were recorded from each surface position, each representing an accumulation of 50 single laser shots spectra. In the right panel of Figure 5 a single measurement campaign at a laser pulse energy of  $\sim 0.5 \mu\text{J}$  is shown, displaying the  $^{34}\text{S}/^{32}\text{S}$  ratio with increasing number of consecutive mass spectra recorded on the same location. This measurement is indicated with a black cross in the Figure 5A (see measurements conducted at  $\sim 0.5 \mu\text{J}$ ). A decrease of the measured  $^{34}\text{S}/^{32}\text{S}$  ratio from about 0.045 to a stable plateau at about 0.027, which involves the very first file number of the measurement up to #20, can be observed. Such a decrease in the ratio was observed for the other measurement as well and is a result of the initial crater formation process in laser ablation. Thus, for data analysis only measurements after stabilization were considered. The start of this stabilization was selected visually and not by applying any statistical measures. Note that the same holds for measurements conducted on the other samples (RT1, RT6, MC, and SC).

In Figure 6 the measurement campaigns conducted on RT1, RT6, MC, and SC are shown. For each sample investigated, a pulse energy campaign was conducted (similar to RT2), and the  $^{34}\text{S}/^{32}\text{S}$  was derived for each applied pulse energy. Interestingly, in each campaign the  $^{34}\text{S}/^{32}\text{S}$  ratio follows a similar trend; first it increases with increasing applied pulse energy, then peaks at a certain pulse energy, and finally decreases back to a lower ratio value. The  $^{34}\text{S}/^{32}\text{S}$  ratio is fitted with a peak function (e.g., a Gram-Charlier peak function) available in the data representation program ORIGIN, and is only displayed to guide the eye; it does not have any scientific meaning.

For the sulphur isotope fractionation calculation  $\delta^{34}\text{S}$  of the three remaining samples (RT1, RT6, and MC) the measured



$^{34}\text{S}/^{32}\text{S}$  ratio maxima were used (**Figure 6**), and calibrated and normalized using the procedure discussed at the end of section *Laser Ablation Ionization Mass Spectrometry*, using the internal standards RT2 and SC. In **Figure 7**, the  $\delta^{34}\text{S}$  values of the investigated samples are plotted, which are internally corrected by the reference sample RT2 and SC (top and bottom values). Blue squares correspond to  $\delta^{34}\text{S}$  values from the state-of-the-art isotope measurements conducted at the Lancaster facilities (**Table 1**), while the black squares correspond to the LIMS measurements using the calculation method described above. The error of the reference measurements are very small and are within the size of the shown symbols. For the LIMS measurements an error at the level of  $\delta^{34}\text{S} \sim 2\%$  was estimated, which matches well the reference measurements. Note that highest deviation was observed for the RT6 sample while for

MC and RT1 an absolute deviation in  $\delta^{34}\text{S}$  of  $\sim 1.3$  and  $0.2$  was derived.

## DISCUSSION

**Figure 4** displays the mass spectra of the investigated samples from Río Tinto, Movile and Sulphur Cave, which are normalized to the major abundant element isotope found within the mass range of  $m/z$  of 5–170. Differences between the identified major and minor element composition of the samples collected at the three different field sites are observed.

The simplest element composition is observed for the sample collected at the Sulphur Cave (SC) site. The spectrum displayed shows that the sample consists mostly of S, three alkali and basic

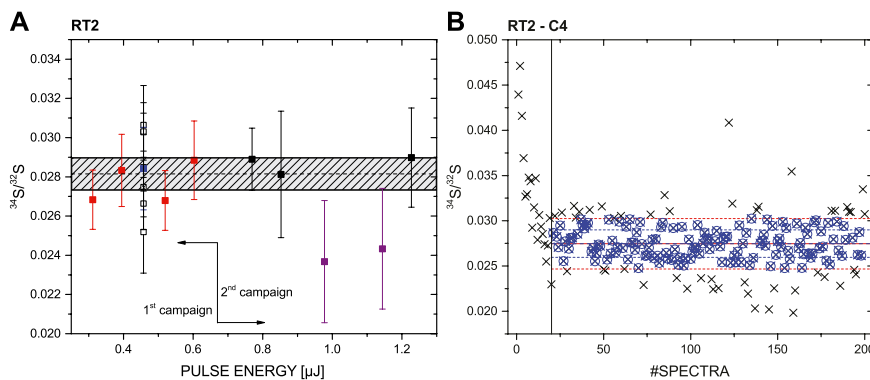


**FIGURE 5** | Measurement campaign conducted on RT2. **(A)**  $^{34}\text{S}/^{32}\text{S}$  ratio for measurements performed with a pulse in the energy range of  $\sim 0.3$ – $1.2$   $\mu\text{J}$ . The blue square is the mean of the measurements conducted at the pulse energy  $\sim 0.5$   $\mu\text{J}$ . The dashed horizontal line represents the mean  $^{34}\text{S}/^{32}\text{S}$  ratio of all conducted measurements excluding the two purple outliers and using the blue square value instead of the individual ones for  $\sim 0.5$   $\mu\text{J}$ ; the dashed grey area represents the mean  $^{34}\text{S}/^{32}\text{S}$  value  $\pm\sigma$ . **(B)** A single measurement campaign conducted at a pulse energy of  $\sim 0.5$   $\mu\text{J}$  (indicated with a black cross in the **(A)**). Spectra at the beginning displaying an elevated  $^{34}\text{S}/^{32}\text{S}$  ratio were not considered for the data analysis.

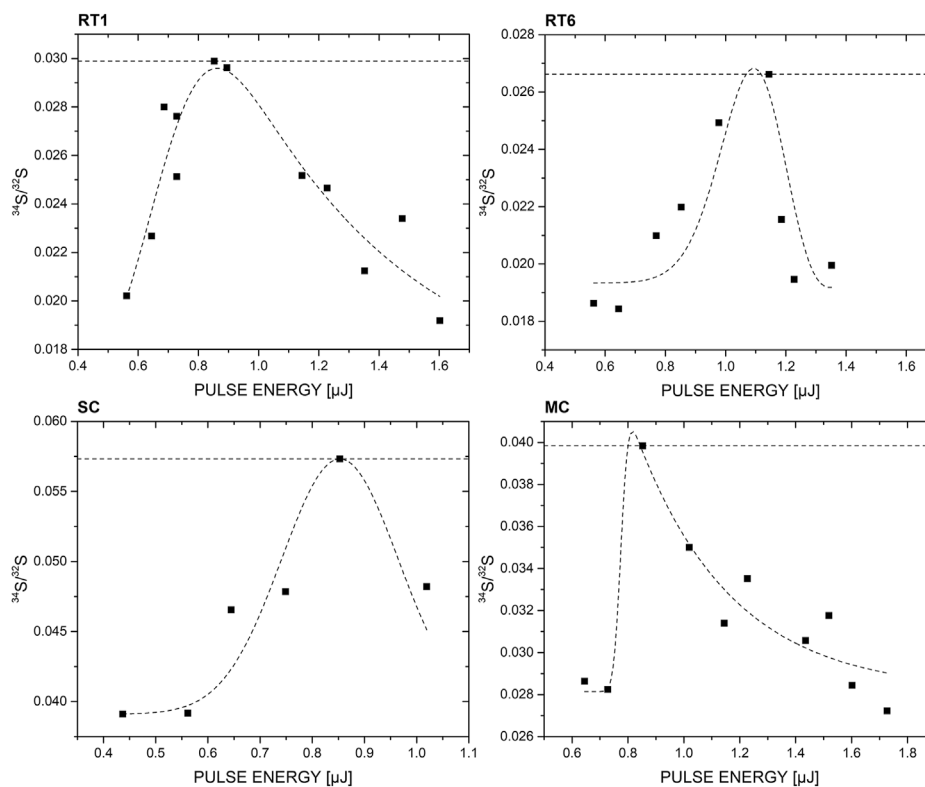
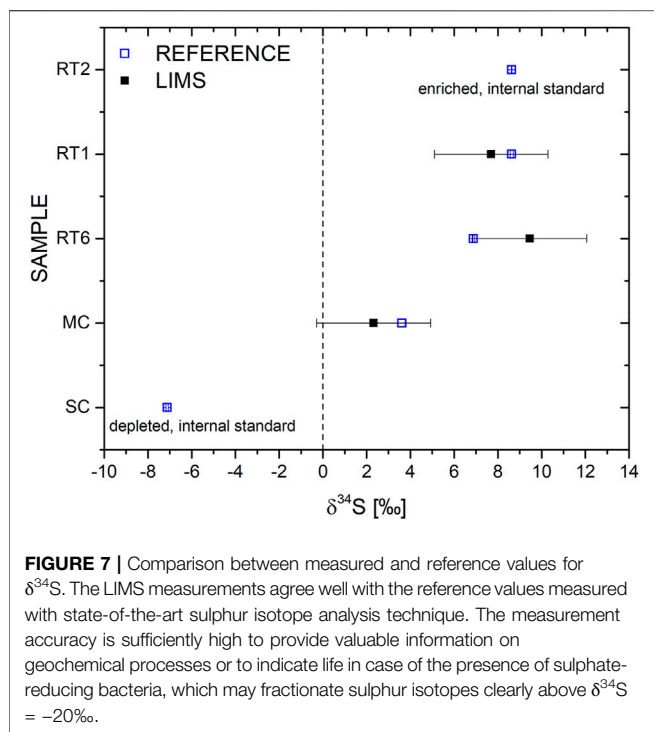


**FIGURE 6** | Correlation between applied pulse energy and  $^{34}\text{S}/^{32}\text{S}$  ratio. For the investigated samples an increase in  $^{34}\text{S}/^{32}\text{S}$  with increasing pulse energy can be observed, peaks at a given pulse energy which is followed by a decrease in ratio. The  $^{34}\text{S}/^{32}\text{S}$  ratio at the peak is comparable to the internal reference measurements conducted on RT2, and allows accurate calculation of the  $\delta^{34}\text{S}$  value of the corresponding sample. Note that the peak like curve is only displayed to guide the eye; it has no scientific value.

metals (Na, K, and Al), and C. The high S content observed in the mass spectrum is in line with the state-of-the-art isotope measurements done at Lancaster facilities, which is at the level of about 97 wt% (see **Table 1** and in comparison to previous studies,

e.g., Sarbu et al., 2018). Due to this high element abundance, various allotropes of S can be identified in the recorded mass spectrum, which can exceed even the structure size of  $\text{S}_6$ . Such molecular structures can easily be formed during the laser ablation process. In



our previous LIMS studies conducted on other sample materials, e.g., high abundant Fe sample, we could identify as well various amounts of single element clusters, with a decreasing signal intensity trend of increasing masses. In this study, we see even the stable  $\text{S}_8$  with increased abundance (see inset showing the  $m/z$  range of 180–270). This observation is in line with mineralogical studies presented in Sarbu et al. (2018). These studies also report the identification of minerals such as potassium-Alum ( $\text{KAl}(\text{SO}_4)_2 \cdot 12\text{H}_2\text{O}$ ) and tamarugite ( $\text{NaAl}(\text{SO}_4)_2 \cdot 6\text{H}_2\text{O}$ ). Therefore, the observed elements K, Al, and Na in our study can be explained by the presence of minor contribution from such minerals. Carbon, on the other hand, can be related to the microbial community within the biofilm, as also discussed by Sarbu et al. (2018).

The recorded mass spectrum of the investigated MC sample shows a slightly richer chemistry. Again, highly abundant S is detected, underlined by the allotropes observed in the spectrum, which is in line with the S isotope measurements at the level of around 15 wt% (Table 1). In comparison to the SC sample, the C abundance in MC is much lower, slightly above the noise level and not visible in the spectrum presented in Figure 4. In contrast, the two elements O and Ti can be observed at minor abundance. Al, Na, and K are as well present with K being the most abundant element in this measurement. The element composition identified in our measurements matches the chemistry observed previously in this cave ecosystem that shows the presence of various minerals, such as clays and calcites (Sarbu et al., 2019).

The richest chemistry is observed for those samples collected from the Río Tinto ecosystem. In addition to the elements measured at the cave systems, metals such as Ti, Mn, Fe, Cu, Zn, and even Ba and BaO could be identified in the recorded mass spectrum. This observation is in agreement with previous studies investigating this

Mars analogue environment, see, e.g., Fernández-Remolar et al., 2005; Amils et al., 2007. Moreover, in comparison to the cave samples, Li can be identified in all three samples easily. Out of the three investigated Río Tinto samples, RT2 is from elemental point of view the most interesting one. It shows the highest abundance of Sulphur (in line with Table 1), and the presence of heavy metallic species, such as Ba, including oxidized Ba.  $\text{Fe}_x\text{S}_y$  clusters up to  $m/z \sim 170$  are detected as well.

In Figure 6, the correlation between the  $^{34}\text{S}/^{32}\text{S}$  ratio and applied laser pulse energy is displayed. The increasing trend on the left side of the peak is attributed to the increasing SNR of the lower abundant  $^{34}\text{S}$  isotope. It requires a certain pulse energy to ablate and ionize sufficient material to see the lower abundant isotope above the measurement noise level. The higher the SNR of the  $^{34}\text{S}$ , the bigger its calculated peak area and consequently the larger the  $^{34}\text{S}/^{32}\text{S}$  ratio. However, this effect holds only to a certain point, therefore the observed maximum. At higher pulse energies, for all samples a decreasing trend can be observed. Various effects contribute to this decrease, including, e.g., space charge and sample charging, and dynamic range of the acquisition system. Note that such a peak-like shape was not observed for RT2, which shows the second highest sulphur abundance. Interestingly, the peak maximum for all four samples occurred at about the same applied pulse energy  $\sim 0.9\text{--}1.1 \mu\text{J}$ , which could be correlated to their similarity in physical (e.g., hardness, colour) and chemical (e.g., composition) characteristics. This might be as well the reason why the NBS 127 isotope standard does not work as internal reference, because it is simply not enough matrix matched, which is important in laser ablation studies. Nevertheless, the  $^{34}\text{S}/^{32}\text{S}$  value at peak maximum allowed the calculation of very accurate  $\delta^{34}\text{S}$  that matched well the reference measurements conducted in Lancaster facilities with the state-of-the-art isotope measurement technique (Table 1).

The achieved and demonstrated  $\delta^{34}\text{S}$  accuracy provides valuable information about both, geochemical and biological processes, that changed the chemical composition of the investigated sample. Sulphate reducing bacteria showed the capability to fractionate the sulphur isotopes up to  $\delta^{34}\text{S} = -70\text{‰}$ , while for geochemical processes an upper limit in fractionation of  $\sim 20\text{‰}$  has so far been observed. Hence, it is important to stress that biotic and abiotic fraction can be differentiated by using our miniature LIMS system. Moreover, the application of the discussed measurement procedure, where a set of pulse energies is tested, is simple and robust, and can be used for *in situ* planetary exploration by adding a simple filter wheel in front of the laser system, in case the laser system itself does not have an internal pulse energy attenuator. Mars would be one of the ideal targets for *in situ* application of our LIMS system. As discussed in detail in, e.g., King and McLennan (2010) or Ding et al. (2015), the sulphur cycle is one of the most important cycles on Mars and provides valuable information on, e.g., geomorphic and aqueous processes, past climate or current habitability on Mars. Local sulphur deposits on the Martian surface can contain up to  $\sim 37$ , and  $\sim 6$  wt% in average, and represent good targets for *in situ* exploration missions using our system. Note, the samples investigated in this study (excluding the SC sample that contains up to  $\sim 96$  wt%) have very comparable sulphur abundances. Further, Martian areas such as the landing site of NASA's Perseverance rover, the Jezero crater, represents other localized areas that are of high interest for life

detection. Such areas were covered in the past with liquid water and therefore represent environments, where life could have flourished for a certain time. Sulphur containing solids in these areas could be investigated by our system and might show indicators of past life, by the identification of an elevated degree of sulphur fractionation ( $\delta^{34}\text{S} > 20$ ).

Sample material collected at three different field sites (Río Tinto in Spain, Movile and Sulphur Caves in Romania) were chemically analyzed using state-of-the-art sulphur isotope measurement instrumentation and a prototype LIMS system for space research. The investigated sample material had sulphur abundances ranging from ~6 wt% to ~96%, with a sulphur fractionation from  $\delta^{34}\text{S} \sim -7$  to +9. The application of a set of pulse energies allowed the identification of  $^{34}\text{S}/^{32}\text{S}$  maxima, which enabled the calculation of  $\delta^{34}\text{S}$  values with accuracies at the ‰, in good agreement with the state-of-art measurement technique. This measurement capability is of high interest to different scientific fields in space exploration, because it provides valuable information on geochemical process but also allows to differentiate between biotic and abiotic fractionation. Furthermore, the determination of the chemical composition of the different samples matched the literature information, demonstrating also its capability for elemental analysis of solids.

## DATA AVAILABILITY STATEMENT

The data supporting the conclusions of this article will be made available by the authors, without undue reservation.

## REFERENCES

- Aerts, J., Röling, W., Elsaesser, A., and Ehrenfreund, P. (2014). Biota and Biomolecules in Extreme Environments on Earth: Implications for Life Detection on Mars. *Life* 4, 535–565. doi:10.3390/life4040535
- Akira, S., Kaoru, H., and Keizo, Y. (1985). Amino Acids from the Yamato-791198 Carbonaceous Chondrite from Antarctica. *Chem. Lett.* 14, 1183–1186. doi:10.1246/cl.1985.1183
- Amils, R., González-Toril, E., Fernández-Remolar, D., Gómez, F., Aguilera, Á., Rodríguez, N., et al. (2007). Extreme Environments as Mars Terrestrial Analogs: The Río Tinto Case. *Planet. Space Sci.* 55, 370–381. doi:10.1016/j.pss.2006.02.006
- Cabedo, V., Llorca, J., Trigo-Rodríguez, J. M., and Rimola, A. (2021). Study of Fischer-tropsch-type Reactions on Chondritic Meteorites. *A&A* 650, A160. doi:10.1051/0004-6361/202039991
- Chela-Flores, J. (2018). Testing S Isotopes as Biomarkers for Mars. *Int. J. Astrobiology* 18 (05), 436–439. doi:10.1017/s1473550418000393
- Chela-Flores, J., Cicuttin, A., Crespo, M. L., and Tuniz, C. (2014). Biogeochemical Fingerprints of Life: Earlier Analogies with Polar Ecosystems Suggest Feasible Instrumentation for Probing the Galilean Moons. *Int. J. Astrobiology* 14, 427–434. doi:10.1017/s1473550414000391
- Chela-Flores, J. (2017). Instrumentation for Testing whether the Icy Moons of the Gas and Ice Giants Are Inhabited. *Astrobiology* 17, 958–961. doi:10.1089/ast.2016.1621
- Chela-Flores, J. (2010). Instrumentation for the Search for Habitable Ecosystems in the Future Exploration of Europa and Ganymede. *Int. J. Astrobiology* 9, 101–108. doi:10.1017/s1473550410000029
- Chela-Flores, J., and Kumar, N. (2008). Returning to Europa: Can Traces of Surficial Life Be Detected? *Int. J. Astrobiology* 7, 263–269. doi:10.1017/s1473550408004242

## AUTHOR CONTRIBUTIONS

AR planned, prepared the sample material, conducted the measurements, including data analysis, and wrote the manuscript. VG supported the measurements and data analysis, and writing of the manuscript. JA provided the sample material and its background information. RLU and MT were involved in writing the manuscript. PB contributed the EDX measurements and supported the writing of the manuscript. RLI provided the facility for sample preparation. PW and PE supported the studies and writing of the manuscript.

## FUNDING

AR acknowledges the financial support of the European Union's Horizon 2020 research and innovation programme under the Marie Skłodowska-Curie grant agreement No. 750353. PW acknowledges the support from the Swiss National Science Foundation.

## ACKNOWLEDGMENTS

AR acknowledges the support from H. Mischler, head of mechanics of the Space Research and Planetary Sciences group of the University Bern, for his support in the preparation of the sample holders used in this study.

- Chela-Flores, J. (2006). The sulphur Dilemma: Are There Biosignatures on Europa's Icy and Patchy Surface? *Int. J. Astrobiology* 5, 17–22. doi:10.1017/s1473550406002862
- Chen, Y., Wu, L., Boden, R., Hillebrand, A., Kumaresan, D., Moussard, H., et al. (2019). Life without Light: Microbial Diversity and Evidence of Sulfur- and Ammonium-Based Chemolithotrophy in Movile Cave. *Isme J.* 3, 1093–1104. doi:10.1038/ismej.2009.57
- Cronin, J. R., and Pizzarello, S. (1983). Amino Acids in Meteorites. *Adv. Space Res.* 3, 5–18. doi:10.1016/0273-1177(83)90036-4
- Ding, S., Dasgupta, R., Lee, C.-T. A., and Wadhwa, M. (2015). New Bulk Sulfur Measurements of Martian Meteorites and Modeling the Fate of Sulfur during Melting and Crystallization - Implications for Sulfur Transfer from Martian Mantle to Crust-Atmosphere System. *Earth Planet. Sci. Lett.* 409, 157–167. doi:10.1016/j.epsl.2014.10.046
- Farquhar, J., Bao, H., and Thiemens, M. (2000). Atmospheric Influence of Earth's Earliest Sulfur Cycle. *Science* 289, 756.
- Farquhar, J., Wing, B. A., McKeegan, K. D., Harris, J. W., Cartigny, P., and Thiemens, M. H. (2002). Mass-Independent Sulfur of Inclusions in Diamond and Sulfur Recycling on Early Earth. *Science* 298, 2369–2372. doi:10.1126/science.1078617
- Farquhar, J., and Wing, B. A. (2003). Multiple Sulfur Isotopes and the Evolution of the Atmosphere. *Earth Planet. Sci. Lett.* 213, 1–13. doi:10.1016/s0012-821x(03)00296-6
- Fernández-Remolar, D. C., Morris, R. V., Gruener, J. E., Amils, R., and Knoll, A. H. (2005). The Río Tinto Basin, Spain: Mineralogy, Sedimentary Geobiology, and Implications for Interpretation of Outcrop Rocks at Meridiani Planum, Mars. *Earth Planet. Sci. Lett.* 240, 149–167. doi:10.1016/j.epsl.2005.09.043
- Grimaudo, V., Moreno-García, P., Riedo, A., Meyer, S., Tulej, M., Neuland, M. B., et al. (2017). Toward Three-Dimensional Chemical Imaging of Ternary Cu-Sn-Pb Alloys Using Femtosecond Laser Ablation/Ionization Mass Spectrometry. *Anal. Chem.* 89, 1632–1641. doi:10.1021/acs.analchem.6b03738

- Grimaudo, V., Moreno-García, P., Riedo, A., Neuland, M. B., Tulej, M., Broekmann, P., et al. (2015). High-Resolution Chemical Depth Profiling of Solid Material Using a Miniature Laser Ablation/Ionization Mass Spectrometer. *Anal. Chem.* 87, 2037–2041. doi:10.1021/ac504403j
- Hand, K. P., Murray, A. E., Garvin, J. B., Brinckerhoff, W. B., Christiner, B. C., Edgett, K. S., et al. (2017). *Report of the European Lander Science Definition Team*. National Aeronautics and Space Administration.
- Kaplan, I. R., and Hulston, J. R. (1966). The Isotopic Abundance and Content of Sulfur in Meteorites. *Geochimica et Cosmochimica Acta* 30, 479–496. doi:10.1016/0016-7037(66)90059-7
- King, P. L., and McLennan, S. M. (2010). Sulfur on Mars. *Elements* 6, 107–112. doi:10.2113/gselements.6.2.107
- Kumaresan, D., Stephenson, J., Doxey, A. C., Bandukwala, H., Brooks, E., Hillebrand-Voiculescu, A., et al. (2018). Aerobic Proteobacterial Methylophiles in Molecule Cave: Genomic and Metagenomic Analyses. *Microbiome* 6, 1. doi:10.1186/s40168-017-0383-2
- Kumaresan, D., Wischer, D., Stephenson, J., Hillebrand-Voiculescu, A., and Murrell, J. C. (2014). Microbiology of Molecule Cave-A Chemolithoautotrophic Ecosystem. *Geomicrobiology J.* 31, 186–193. doi:10.1080/01490451.2013.839764
- Martins, Z., Alexander, C. M. O. D., Orzechowska, G. E., Fogel, M. L., and Ehrenfreund, P. (2007a). Indigenous Amino Acids in Primitive CR Meteorites. *Meteoritics Planet. Sci.* 42, 2125–2136. doi:10.1111/j.1945-5100.2007.tb01013.x
- Martins, Z., Hofmann, B. A., Gnos, E., Greenwood, R. C., Verchovsky, A., Franchi, I. A., et al. (2007b). Amino Acid Composition, Petrology, geochemistry, 14C Terrestrial Age and Oxygen Isotopes of the Shīr 033 CR Chondrite. *Meteoritics Planet. Sci.* 42, 1581–1595. doi:10.1111/j.1945-5100.2007.tb00592.x
- Meyer, S., Riedo, A., Neuland, M. B., Tulej, M., and Wurz, P. (2017). Fully Automatic and Precise Data Analysis Developed for Time-Of-Flight Mass Spectrometry. *J. Mass. Spectrom.* 52, 580–590. doi:10.1002/jms.3964
- Neubeck, A., Tulej, M., Ivarsson, M., Broman, C., Riedo, A., McMahon, S., et al. (2015). Mineralogical Determination *In Situ* of a Highly Heterogeneous Material Using a Miniaturized Laser Ablation Mass Spectrometer with High Spatial Resolution. *Int. J. Astrobiology* 15, 133–146. doi:10.1017/s1473550415000269
- Orosei, R., Lauro, S. E., Pettinelli, E., Cicchetti, A., Coradini, M., Cosciotti, B., et al. (2018). Radar Evidence of Subglacial Liquid Water on Mars. *Science* 361, 490–493. doi:10.1126/science.aar7268
- Riedo, A., Bieler, A., Neuland, M., Tulej, M., and Wurz, P. (2013a). Performance Evaluation of a Miniature Laser Ablation Time-Of-Flight Mass Spectrometer Designed For *In Situ* Investigations in Planetary Space Research. *J. Mass. Spectrom.* 48, 1–15. doi:10.1002/jms.3104
- Riedo, A., Koning, C. d., Stevens, A., McDonald, A., López, A. C., Tulej, M., et al. (2020). The Detection of Microbial Life Fingerprint in Martian Mudstone Analogues Using High Spatially Resolved Laser Ablation Ionization Mass Spectrometry. *Astrobiology*. in press.
- Riedo, A., Lukmanov, R., Grimaudo, V., de Koning, C., Ligterink, N. F. W., Tulej, M., et al. (2021). Improved Plasma Stoichiometry Recorded by LIMS by Using a Double-Pulse Femtosecond Laser Ablation Ion Source. *Rapid Commun. Mass Spectrom.* in press.
- Riedo, A., Neuland, M., Meyer, S., Tulej, M., and Wurz, P. (2013b). Coupling of LIMS with a Fs-Laser Ablation Ion Source: Elemental and Isotope Composition Measurements. *J. Anal. Spectrom.* 28, 1256–1269. doi:10.1039/c3ja50117e
- Rotelli, L., Trigo-Rodríguez, J. M., Moyano-Camero, C. E., Carota, E., Botta, L., Di Mauro, E., et al. (2016). The Key Role of Meteorites in the Formation of Relevant Prebiotic Molecules in a Formamide/water Environment. *Sci. Rep.* 6, 38888. doi:10.1038/srep38888
- Sarbu, S., Aerts, J. W., Aerts, J., Flot, J.-F., Van Spanning, R., Baciu, C., et al. (2018). Sulfur Cave (Romania), an Extreme Environment with Microbial Mats in a CO<sub>2</sub>-H<sub>2</sub>S/O<sub>2</sub> Gas Chemocline Dominated by Mycobacteria. *Ijs* 47, 173–187. doi:10.5038/1827-806x.47.2.2164
- Sarbu, S. M., Lascu, C., and Brad, T. (2019). “Dobrogea: Molecule Cave,” in *Cave and Karst Systems of Romania GML Ponta and BP Onacs* (Cham: Springer International Publishing), 429–436. doi:10.1007/978-3-319-90747-5\_48
- Shearer, C. K., Layne, G. D., Papike, J. J., and Spilde, M. N. (1996). Sulfur Isotopic Systematics in Alteration Assemblages in Martian Meteorite Allan Hills 84001. *Geochimica et Cosmochimica Acta* 60, 2921–2926. doi:10.1016/0016-7037(96)00165-2
- Stevens, A. H., McDonald, A., de Koning, C., Riedo, A., Preston, L. J., Ehrenfreund, P., et al. (2019). Detectability of Biosignatures in a Low-Biomass Simulation of Martian Sediments. *Sci. Rep.* 9, 9706. doi:10.1038/s41598-019-46239-z
- Trigo-Rodríguez, J. M., Lee, M. R., and Leroux, H. (2015). “Aqueous Alteration in Chondritic Asteroids and Comets from the Study of Carbonaceous Chondrites,” in *Planetary Mineralogy* (Aberystwyth, UK: Cambrian Press). doi:10.1180/emu-notes.15.3
- Tulej, M., Ligterink, N. F. W., de Koning, C., Grimaudo, V., Lukmanov, R., Keresztes Schmidt, P., et al. (2021). Current Progress in Femtosecond Laser Ablation/Ionisation Time-Of-Flight Mass Spectrometry. *Appl. Sci.* 11, 2562. doi:10.3390/app11062562
- Tulej, M., Neubeck, A., Ivarsson, M., Riedo, A., Neuland, M. B., Meyer, S., et al. (2015). Chemical Composition of Micrometer-Sized Filaments in an Aragonite Host by a Miniature Laser Ablation/Ionization Mass Spectrometer. *Astrobiology* 15, 669–682. doi:10.1089/ast.2015.1304
- Tulej, M., Wiesendanger, R., Riedo, A., Knopp, G., and Wurz, P. (2018). Mass Spectrometric Analysis of the Mg Plasma Produced by Double-Pulse Femtosecond Laser Irradiation. *J. Anal. Spectrom.* 33, 1292–1303. doi:10.1039/c8ja00036k
- Visser, R., John, T., Patzek, M., Bischoff, A., and Whitehouse, M. J. (2019). Sulfur Isotope Study of Sulfides in CI, CM, C2ung Chondrites and Volatile-Rich Clasts - Evidence for Different Generations and Reservoirs of Sulfide Formation. *Geochimica et Cosmochimica Acta* 261, 210–223. doi:10.1016/j.gca.2019.06.046
- Wiesendanger, R., Wacey, D., Tulej, M., Neubeck, A., Ivarsson, M., Grimaudo, V., et al. (2018). Chemical and Optical Identification of Micrometer-Sized 1.9 Billion-Year-Old Fossils by Combining a Miniature Laser Ablation Ionization Mass Spectrometry System with an Optical Microscope. *Astrobiology* 18, 1071–1080. doi:10.1089/ast.2017.1780
- Wynn, P. M., Loader, N. J., and Fairchild, I. J. (2014). Interrogating Trees for Isotopic Archives of Atmospheric sulphur Deposition and Comparison to Speleothem Records. *Environ. Pollut.* 187, 98–105. doi:10.1016/j.envpol.2013.12.017

**Conflict of Interest:** The authors declare that the research was conducted in the absence of any commercial or financial relationships that could be construed as a potential conflict of interest.

**Publisher’s Note:** All claims expressed in this article are solely those of the authors and do not necessarily represent those of their affiliated organizations, or those of the publisher, the editors and the reviewers. Any product that may be evaluated in this article, or claim that may be made by its manufacturer, is not guaranteed or endorsed by the publisher.

Copyright © 2021 Riedo, Grimaudo, Aerts, Lukmanov, Tulej, Broekmann, Lindner, Wurz and Ehrenfreund. This is an open-access article distributed under the terms of the Creative Commons Attribution License (CC BY). The use, distribution or reproduction in other forums is permitted, provided the original author(s) and the copyright owner(s) are credited and that the original publication in this journal is cited, in accordance with accepted academic practice. No use, distribution or reproduction is permitted which does not comply with these terms.